Available online at www.sciencedirect.com

SciVerse ScienceDirect

Ceramics International 39 (2013) 6287–6291

CERAMICS INTERNATIONAL

www.elsevier.com/locate/ceramint

In situ growth of hydroxyapatite on lamellar alumina scaffolds with aligned pore channels

Luyang Hu[a,*], Yumin Zhang[b], Shanliang Dong[b], Shanmei Zhang[c], Benxia Li[a]

[a]School of Materials Science and Engineering, Anhui University of Science & Technology, Huainan 232001, China
[b]Center for Composite Materials, Harbin Institute of Technology, Harbin 150001, China
[c]School of Science, Anhui University of Science & Technology, Huainan 232001, China

Received 29 October 2012; received in revised form 15 January 2013; accepted 16 January 2013
Available online 1 February 2013

Abstract

We prepared hydroxyapatite/alumina (HA/Al_2O_3) porous composite materials by the in situ growth of HA on lamellar Al_2O_3 ceramics. The procedure comprises two steps. First, lamellar Al_2O_3 ceramics with aligned pore channels were obtained by freeze casting Al_2O_3 slurry. Second, as-prepared monoliths were used as scaffolds and subjected to hydrothermal treatment in the HA precursor solution. We characterized the microstructure, chemical composition, and mechanical properties of synthesized HA/Al_2O_3. Experiment results show that the addition of H_2O_2 into the reaction solution plays an important role in controlling the microstructure of the cultivated HA. The formation of HA has no obvious influence on the lamellar architecture of Al_2O_3 ceramics. The prepared composite materials exhibit superior compressive strength. Combination of the high strength of lamellar Al_2O_3 with the excellent biological properties of HA increases the potential of obtained HA/Al_2O_3 for load-bearing biological applications.

Keywords: B. Microstructure-final; C. Strength; HA/Al_2O_3; In situ growth

1. Introduction

Hydroxyapatite (HA) is a very attractive material for biomedical applications because of its excellent biocompatibility, bioactivity, and osteoconductivity [1]. Porous HA improves bone ingrowth and osseointegration, thus, it is highly suitable as bone scaffold material [2]. However, the inherent lack of strength associated with porosity limits its application, particularly in the cases where load-bearing is required [3]. The freeze-casting technique was developed to improve the mechanical properties of HA. This method enables lamellar porous structures with homogeneous and well-defined architectures to be obtained [3,4]. However, these porous structures do not fully meet the load-bearing requirements [3]. The main reason comes from the poor strength of pure HA [5]. An alternative method to solve this problem is to composite HA into a porous material. For example, Kim et al. [6] used porous ZrO_2 ceramics as supporting carriers, and then coated an HA layer on the ZrO_2 scaffolds to obtain a composite material with high mechanical properties. However, high sintering temperature is required to prepare such materials. This type of temperature will induce the decomposition of HA [7,8] or the chemical reaction between HA and carrier [6], thus reducing the biocompatibility of the material [6]. To avoid the decomposition or reaction, HA can be directly cultivated on a porous carrier by hydrothermal approach [9,10].

In this paper, we introduce a lamellar Al_2O_3 scaffold with aligned pore channels as a supporting material, and then cultivated the HA on the ceramic scaffold by hydrothermal method. Previous research reveals that Al_2O_3 ceramic prepared by freeze-casting possesses high compressive strength [11,12], whereas the hydrothermal process does not significantly change the microstructure of the supporting material [9,10]. The prepared porous HA/Al_2O_3 composite scaffold will strengthen the potential of HA for load-bearing biological applications. We illustrated in subsequent sections of the paper how freeze casting and hydrothermal treatment are used in the fabrication of a bone substitute material. The obtained

*Corresponding author. Tel./Fax: 86 554 6668 643.
E-mail address: Huluyang2005@yahoo.com.cn (L. Hu).

0272-8842/$ - see front matter © 2013 Elsevier Ltd and Techna Group S.r.l. All rights reserved.
http://dx.doi.org/10.1016/j.ceramint.2013.01.050

samples were characterized by evaluating XRD patterns, FTIR spectra, microstructures, and the mechanical properties of these materials.

2. Experimental procedure

Commercially available alumina powder (99.99% α-Al_2O_3, mean particle size 0.4 μm, Dalian Luming Nanometer Material Co., Ltd., Dalian, China) was used to produce a composite ceramic. An aqueous suspension at a solids loading of 20 vol% was prepared by mixing ceramic powder, Darvan 7-N (dispersant, 1.2 wt% of the powder, R.T. Vanderbilt Co., Connecticut, US), and glycerol (10 wt% of the solvent) into distilled water. The mixture was then milled for 24 h with zirconia balls (6 mm, the mass ratio of balls and powder is 3:1) as the ball-milled media at a rotation speed of 120 rpm. The resulting suspension was poured into a polyethylene mold (40 mm diameter, 15 mm long) and placed on refrigerated equipment (−20 °C), similar to that designed by Fukasawa et al. [13], to induce the unidirectional solidification of the slurry from the bottom to the top. As the freezing process was completed (~12 min), the frozen sample was freeze-dried at −40 °C and <10 Pa (Freeze Dryer, Beijing SongYuan Huaxing Technology Development Co. Ltd., China), for 48 h to remove solvent. The green part was sintered in air for 4 h at 1500 °C at a constant rate of 5 °C/min, followed by naturally cooling in furnace to room temperature.

After sintering, 5 mm × 5 mm × 8 mm cubes were removed from the porous Al_2O_3 sample and then washed three times in ethanol with sonication. The dried cubes were immersed into a 50 ml Teflon-lined vessel containing 0.12 M $Ca(NO_3)_2 \cdot 4H_2O$ (Analytical Reagent [AR]), 0.072 M $NH_4H_2PO_4$ (AR), 0.36 M urea (AR), 1.5 M H_2O_2 (AR). The hydrothermal reaction was conducted at 150 °C for 3 h, followed by natural cooling to room temperature. Finally, recovered composite scaffolds were washed with distilled water to remove the loosely adsorbed material and then dried in air. These samples are referred to as AH1. Following the above steps for AH1, another reaction was conducted in the absence of H_2O_2, and the obtained materials for this reaction are referred to as AH2.

The as-prepared products were observed by an environmental scanning electron microscope (XL30 ESEM TMP, Philips-FEI Corp., Holand). The X-ray diffraction patterns were recorded on an X-ray diffractometer with Cu Kα radiation (XRD 6000, Shimadzu Corp., Japan). The powder sample scratched from AH1 or AH2 was mixed with KBr and pressed into a pellet for FTIR measurement (Nicolet 380, Thermo electron corp., U.S.), respectively. The apparent density and porosity of Al_2O_3, AH1 and AH2 were measured using the Archimedes method. Test samples were loaded at a testing machine (Instron 5569, Instron corp., Canton, U.S.) to measure the compressive strengths at a crosshead speed of 1 mm/min. More than six samples were used for each measurement to obtain the average value.

3. Results and discussion

The microstructure of prepared porous alumina ceramic is shown in Fig. 1. The sample exhibits a mesh-like morphology

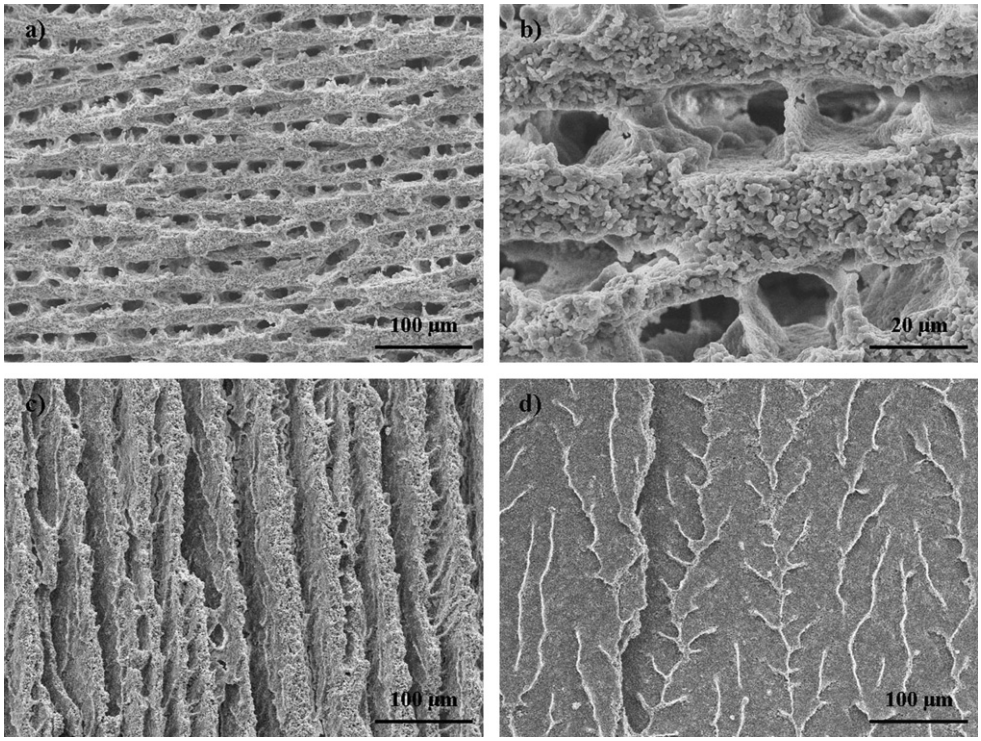

Fig. 1. SEM micrographs of the porous alumina ceramic support. (a) and (b) cross section; (c) vertical section; (d) lamellae surface.

in the parallel direction of the ice front (Fig. 1a and b), which is similar to that observed in previous report [12]. The average pore size, measured by using an intercept method, is 19 μm. In the perpendicular direction of the ice front, the porous ceramic obviously displays a lamellar architecture (Fig. 1c). Some dendriticlike parts protrude on the surface of these lamellae (Fig. 1d) and even extend to neighboring lamella walls (Fig. 1b). This favorable lamellar structure and connections between lamellae endue the porous Al_2O_3 ceramic with high mechanical properties (Table 1). When the porosity is 64.3%, the compressive strength reaches 116.6 MPa (Table 1). This value is much higher than that of the porous HA ceramic obtained by freeze casting [3].

After the hydrothermal treatment, lamellar architectures of the porous supporting materials were well preserved. A white deposition on the exterior of the alumina substrate was observed. The relevant SEM images are shown in Fig. 2. When H_2O_2 is present in the hydrothermal reaction system, the deposition is constructed by a large number of flower-like and stick-like agglomerates (Fig. 2a and b). By contrast, only a few stick-like and fiber-like agglomerates are dispersed on the external surface of the substrate in the absence of H_2O_2 (Fig. 2c and d). The difference micrographs may indicate that the presence of H_2O_2 is beneficial to the densification and microstructure transition of deposition growth on exterior domain of the alumina ceramic, as reported by Nayak et al. [14].

In order to identify phases of the composite materials, the XRD patterns of prepared scaffolds and the FTIR patterns of the scratched powder are shown in Fig. 3. It is seen clearly that the prepared samples can be well indexed with HA (JCPDS 09-0432) and Al_2O_3 (JCPDS 46-1212), and no other phases are found in the composite materials (Fig. 3a). Comparing with AH1, some diffraction peaks of HA (remarked with the filled inverted triangle) disappear in the XRD pattern of AH2. This may be due to the microstructure changes of HA on the exterior surface of the alumina substrate. In the FTIR patterns, a set of absorption peaks can be observed (Fig. 3b). The peaks at 1034, 1108, 960, 566, 604, and 470 cm^{-1} correspond to the characteristic bands of PO_4^{3-} [15]. The peaks at 3566 and 633 cm^{-1} are ascribed to the stretching and librational modes of the structural OH^- in HA [16]. Moreover, the broad peaks attributed to OH group of adsorbed water are

Table 1
Properties of the alumina ceramic and the composite scaffolds.

Sample	Apparent density (g/cm^3)	Porosity (%)	Compressive strength (MPa)
Al_2O_3	1.421 ± 0.025	64.3 ± 0.6	116.6 ± 2.3
AH1	1.434 ± 0.028	63.9 ± 0.7	110.3 ± 2.5
AH2	1.427 ± 0.024	64.1 ± 0.6	107.1 ± 2.4

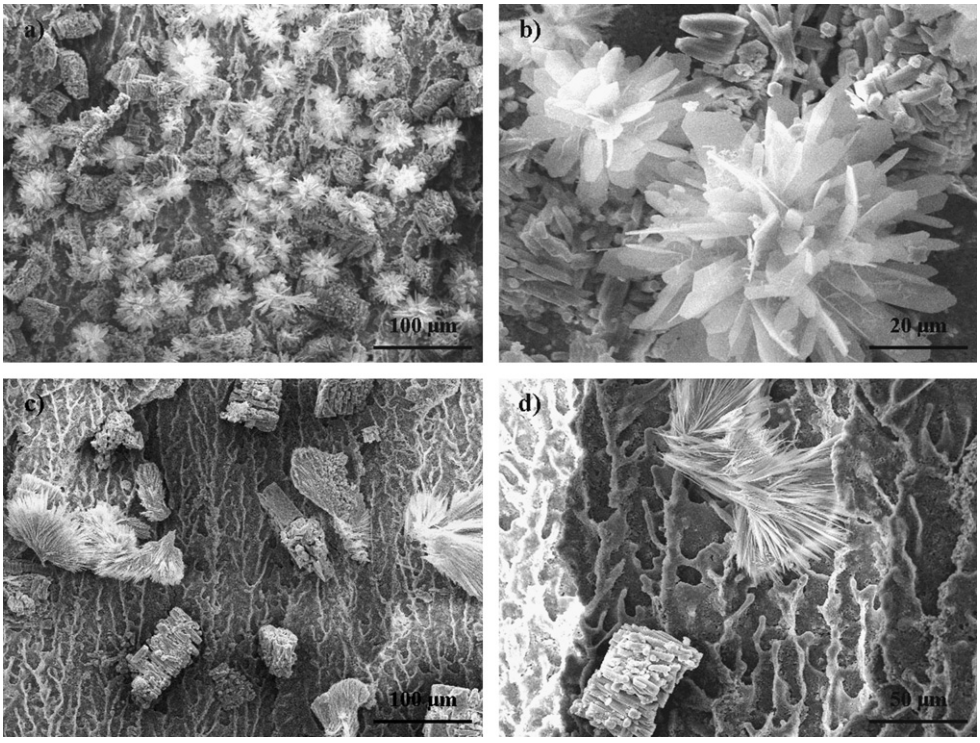

Fig. 2. Microstructure on the exterior surface of alumina substrate. (a) and (b) AH1; (c) and (d) AH2.

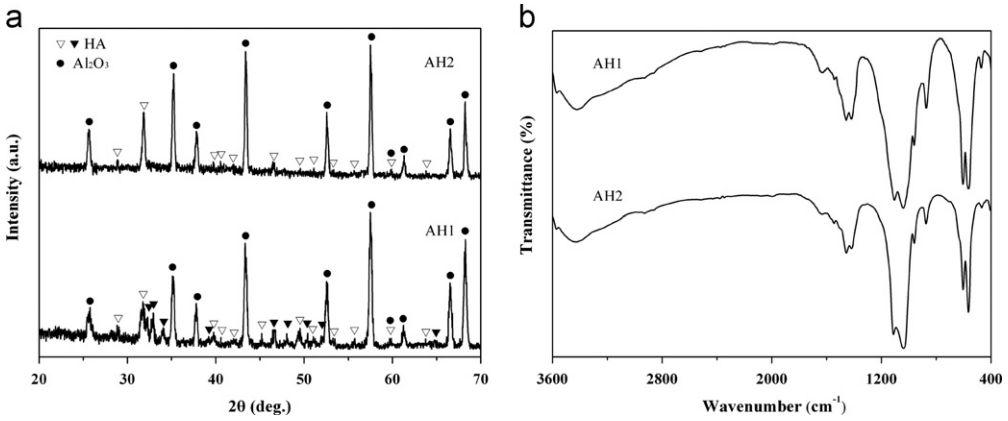

Fig. 3. (a) XRD patterns of the prepared composites scaffolds; (b) FTIR spectra of the cultivated HA.

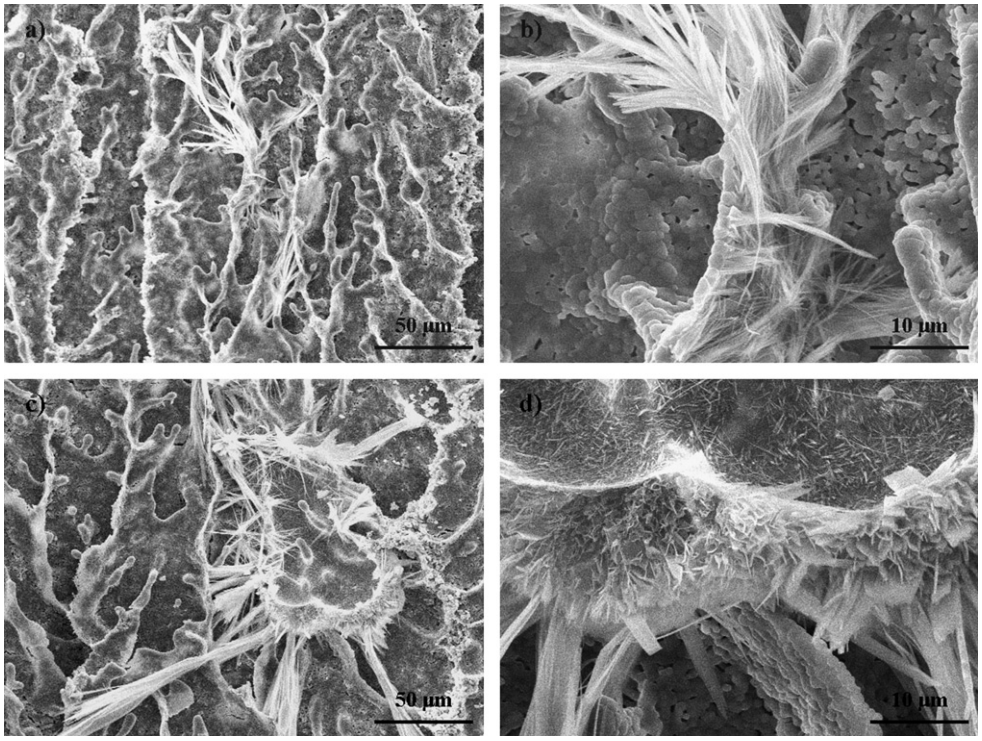

Fig. 4. Microstructure on the interior surface of the alumina substrate. (a) and (b) AH1; (c) and (d) AH2.

also detected with a center at 3420 and 1633 cm^{-1}. Considering that decomposed urea forms CO_2 and aqueous ammonia in hydrothermal treatment, a part of carbon dioxide can perhaps be transformed into CO_3^{2-} [16]. Thus, the presence of peaks at 1542 cm^{-1} (CO_3^{2-} for OH^-, A-type substitution), 1453, 1414 and 873 cm^{-1} (CO_3^{2-} for PO_4^{3-}, B-type substitution) [17] indicate that the deposition of AH1 and AH2 on alumina ceramic is carbonated HA.

The microstructure of HA on the internal surface of the alumina substrate is completely different from that on the exterior surface, as shown in Fig. 4. This difference can perhaps be attributed to the mass transfer limitation or/and low-amount of HA precursor solution in the porous structure of the substrate. In the AH1 sample, HA displays a fiber-like agglomerates structure (Fig. 4a) and the HA nanofibers grow on protruded dendriticlike parts of the alumina (Fig. 4b). In the AH2 sample, the fiber-like and sheet-like HA conglomerates are cultivated on the lamella of the alumina (Fig. 4c and d). Some HA nanofibers and ribbons germinate from conglomerates (Fig. 4c). These exotic morphologies are not found on the surface of porous carbon [9] and TiO_2 nanotube arrays [10].

Although HA propagated on the surface of the alumina ceramic after hydrothermal reaction, the porosity and compressive strength of the prepared composite scaffolds do not exhibit obvious changes compared with those of the substrate (Table 1). This result may indicate that the supporting scaffold by the hydrothermal treatment can increase its biological properties, while mechanical and physical properties of that

are maintained. Therefore, the prepared AH1 and AH2 will perhaps be expected as bone substitute to apply in load-bearing biological tissue engineering.

4. Conclusions

Two HA/Al_2O_3 porous composite scaffolds with high compress strength were prepared by the hydrothermal treatment process using lamellar alumina ceramics with aligned pore channels as the supporting materials. For both samples, the XRD and SEM results showed that HA was synthesized on the surface of the alumina substrate. When 1.5 M H_2O_2 was added to HA precursor solution, the deposition on the exterior of the alumina was evidently increased, and fiber-like and sheet-like HA conglomerates on the internal surface of the alumina substrate were changed into fiber-like agglomerates structure. Furthermore, the presence of AB-type substitution in the formed HA was also revealed by the FTIR measurement.

Acknowledgments

The author would like to thank Dr. Zehui Jiang for reviewing the manuscript. This work was supported by the National Natural Science Foundation of China (No. 51208003 and No. 21001003), the Key Laboratory Opening Funding of the National Key Laboratory of Science and Technology on Advanced Composites in Special Environment and the introduced doctor's startup fund from the Anhui University of Science and Technology.

References

[1] A. Lak, M. Mazloumi, M. Mohajerani, A. Kajbafvala, S. Zanganeh, H. Arami, S.K. Sadrnezhaad, Self-assembly of dandelion-like hydroxyapatite nanostructures via hydrothermal method, Journal of the American Ceramic Society 91 (2008) 3292–3297.

[2] H. Kim, J.C. Knowles, H. Kim, Hydroxyapatite/poly(ε-caprolactone) composite coatings on hydroxyapatite porous bone scaffold for drug delivery, Biomaterials 25 (2004) 1279–1287.

[3] S. Deville, E. Saiz, A.P. Tomsia, Freeze casting of hydroxyapatite scaffolds for bone tissue engineering, Biomaterials 27 (2006) 5480–5489.

[4] S. Deville, E. Saiz, R.K. Nalla, A.P. Tomsia, Freezing as a path to build complex composites, Science 311 (2006) 515–518.

[5] G. Singh, S. Singh, S. Prakash, Surface characterization of plasma sprayed pure and reinforced hydroxyapatite coating on Ti_6Al_4V alloy, Surface and Coatings Technology 205 (2011) 4814–4820.

[6] H. Kim, S. Lee, C. Bae, Y. Noh, H. Kim, H. Kim, J.S. Ko, Porous ZrO_2 bone scaffold coated with hydroxyapatite with fluorapatite intermediate layer, Biomaterials 24 (2003) 3277–3284.

[7] Z. Evis, R.H. Doremus, Effect of ZrF_4 on hot-pressed hydroxyapatite/monoclinic zirconia composites, Scripta Materialia 56 (1) (2007) 53–57.

[8] S. Nath, K. Biswas, B. Basu, Phase stability and microstructure development in hydroxyapatite-mullite system, Scripta Materialia 58 (2008) 1054–1057.

[9] H. Liu, L. Xia, Y. Dai, M. Zhao, Z. Zhou, H. Liu, Fabrication and characterization of novel hydroxyapatite/porous carbon composite scaffolds, Materials Letters 66 (2012) 36–38.

[10] X. Lu, H. Zhang, Y. Guo, Y. Wang, X. Ge, Y. Leng, F. Watari, Hexagonal hydroxyapatite formation on TiO_2 nanotubes under urea modulation, CrystEngComm 13 (2011) 3741–3749.

[11] J. Han, L. Hu, Y. Zhang, Y. Zhou, Fabrication of ceramics with complex porous structures by the impregnate-freeze-casting process, Journal of the American Ceramic Society 92 (2009) 2165–2167.

[12] Y. Zhang, L. Hu, J. Han, Z. Jiang, Freeze casting of aqueous alumina slurries with glycerol for porous ceramics, Ceramics International 36 (2010) 617–621.

[13] T. Fukasawa, M. Ando, T. Ohji, S. Kanzaki, Synthesis of porous ceramics with complex pore structure by freeze-dry processing, Journal of the American Ceramic Society 84 (2001) 230–232.

[14] S. Nayak, B. Satpati, R.K. Shukla, A. Dhawan, S. Bhattacharjee, Y.S. Chaudhary, Facile synthesis of nanostructured hydroxyapatite-titania bio-implant scaffolds with different morphologies: their bioactivity and corrosion behaviour, Journal of Materials Chemistry 20 (2010) 4949–4954.

[15] K. Lin, Y. Zhou, Y. Zhou, H. Qu, F. Chen, Y. Zhu, J. Chang, Biomimetic hydroxyapatite porous microspheres with co-substituted essential trace elements: surfactant-free hydrothermal synthesis, enhanced degradation and drug release, Journal of Materials Chemistry 21 (2011) 16558–16565.

[16] I.S. Neira, Y.V. Kolen'ko, O.I. Lebedev, G.V. Tendeloo, H.S. Gupta, F. Guitian, M. Yoshimura, An effective morphology control of hydroxyapatite crystals via hydrothermal synthesis, Crystal Growth and Design 9 (2009) 466–474.

[17] H. Morgan, R.M. Wilson, J.C. Elliott, S.E.P. Dowker, P. Anderson, Preparation and characterisation of monoclinic hydroxyapatite and its precipitated carbonate apatite intermediate, Biomaterials 21 (2000) 617–627.